

Imprints of Molecular Clouds in Radio Continuum Images

F. Yusef-Zadeh

Department of Physics and Astronomy Northwestern University, Evanston, Il. 60208

ABSTRACT

We show radio continuum images of several molecular complexes in the inner Galaxy and report the presence of dark features that coincide with dense molecular clouds. Unlike infrared dark clouds, these features which we call “radio dark clouds” are produced by a deficiency in radio continuum emission from molecular clouds that are embedded in a bath of UV radiation field or synchrotron emitting cosmic ray particles. The contribution of the continuum emission along different pathlengths results in dark features that trace embedded molecular clouds. The new technique of identifying cold clouds can place constraints on the depth and the magnetic field of molecular clouds when compared to those of the surrounding hot plasma radiating at radio wavelengths. The study of five molecular complexes in the inner Galaxy, Sgr A, Sgr B2, radio Arc, the snake filament and G359.75-0.13 demonstrate an anti-correlation between the distributions of radio continuum and molecular line and dust emission. Radio dark clouds are identified in GBT maps and VLA images taken with uniform sampling of uv coverage. The level at which the continuum flux is suppressed in these sources suggests that the depth of the molecular cloud is similar to the size of the continuum emission within a factor of two. These examples suggest that high resolution, high dynamic range continuum images can be powerful probes of interacting molecular clouds with massive stars and supernova remnants in regions where the kinematic distance estimates are ambiguous as well as in the nuclei of active galaxies.

Subject headings: ISM: clouds —molecules —structure Galaxy: center

1. Radio Dark Clouds

The inner few degrees of the Galactic center show a large concentration of molecular, atomic hydrogen and dust clouds (Pierce-Price et al. 2000; Lang et al. 2010; Molinari et al. 2011). The molecular gas toward the Galactic center is considered to reside in the so-called central molecular zone (CMZ) and consists of a mixture of diffuse and dense components

(Morris and Serabyn 1996; Martin et al. 2004; Sawada et al. 2004; Oka et al. 2005; Yusef-Zadeh et al. 2012). Radio continuum emission from this region is also extended and is produced by a mixture of thermal and nonthermal processes (Nord et al. 2004; Yusef-Zadeh et al. 2004; Law et al. 2008). Given the confusing region of the inner Galaxy due to large number of foreground and background sources along the line of sight as well as the complex motion of the gas in the Galactic center, it is difficult to use the kinematic distance method to identify molecular clouds associated with HII regions and supernova remnants. We describe a new technique to identify neutral clouds that show a deficiency in the distribution of radio continuum emission. These clouds are embedded in a bath of radiation or cosmic ray particles produced by thermal or nonthermal sources, respectively. The strong radiation field in the environment of cloud complexes with high column densities, such as Infrared Dark Clouds (IRDCs), allow us to identify their dark counterparts in radio continuum images at cm and mm wavelengths.

The origin of radio dark clouds (RDCs) is unlike the X-ray shadowing and IRDCs which are caused by strong absorption of background light by dense clouds (Egan et al. 1998; Andersen et al. 2010). RDCs are also unlike optically thick HII regions seen in absorption against the strong background nonthermal emission at low frequencies. This effect is due to a free-free absorption coefficient which increases at low frequencies as $\nu^{-2.1}$ (Nord et al. 2004). The origin of the deficiency in radio continuum emission at high frequencies is due to the high column of embedded molecular gas that does not allow an external radiation field or cosmic ray particles to penetrate through the cloud. This implies that this subset of molecular clouds is interacting with its surrounding hot medium. We first demonstrate the physical situation in which radio dark clouds are produced followed by five examples demonstrating the reality of radio dark clouds.

Since background radio continuum radiation is transparent when passing through neutral clouds, one would expect uniform background emission across the face of neutral clouds. However, if a cloud is surrounded by hot synchrotron or thermal emitting plasma, the continuum emission is depressed due to the shorter path length of the continuum emission integrated along the line of sight toward the center of the molecular cloud. One possibility involves external heating and ionization of neutral gas by ultraviolet continuum radiation that falls off rapidly from the edge to the center of the cloud with where the visual extinction (A_v) is much larger than one magnitude. Thus, free-free radio emission is substantially reduced in clouds with high column densities and their imprint can be identified as dark features in radio continuum images. In other words, atomic or molecular gas clouds or dust clouds suppress the continuum emission and create the appearance of a "hole" in their distribution. It is expected that neutral clouds embedded in a hot plasma are edge brightened outlining the boundary of the cloud, thus can be distinguished from a cavity devoid of gas.

The presence of spectral line and/or continuum dust emission can also distinguish RDCs.

We consider a cloud with a diameter d located at a distance D from us and is embedded within an ionized medium characterized to have electron density n_e (cm^{-3}) and with the emission measure $E_l = n_e^2 l \text{ cm}^{-6} \text{ pc}$ along a path length l . The surface brightness toward the center and away from the cloud are defined as $S_{\nu,d}$ and $S_{\nu,l}$, respectively, at a given frequency ν . The flux deficiency ΔS_ν is the difference between the flux density of the ambient gas toward and away from the cloud. The ratio of the diameter of the cloud to the path length l is

$$\frac{d}{l} = \frac{\Delta S_\nu}{S_{\nu,l}} \quad (1)$$

The differential emission measure ΔEM between the cloud center and the ionized medium can be estimated by

$$\Delta EM = \frac{2.15 \times 10^2 \Delta S_\nu \nu^{0.1} T_e^{0.35}}{\theta^2} = n_e^2 d \text{ pc cm}^{-6} \quad (2)$$

where T_e is the electron temperature in K, θ is the beam size in arcsecond and ΔS_ν is the flux deficiency in mJy. If the electron density of the ionized medium is measured independently, then the depth of the molecular cloud d along the line of sight can be estimated.

Another possibility that could produce RDCs is the deflection of non-thermal particles as they diffuse inside a molecular cloud. In this case, the path length over which nonthermal particles travel are limited by the magnetic field geometry of the cloud which could shield the electrons penetrating into the cloud. The ionization losses of nonthermal particles could also suppress the emission from high energy particles as they interact with the gas. Thus, the flux of nonthermal emission at high frequencies is expected to be reduced with respect to the background nonthermal emission. If we assume that the magnetic field is in equipartition with the particles, the ratio of the magnetic field in the diffuse medium to the molecular cloud is

$$\frac{B_l}{B_d} = \left(\frac{S_{\nu,l} \times (l - d)}{S_{\nu,d} \times l} \right)^{\frac{1}{3+\alpha}} \quad (3)$$

where B_l and B_d are the magnetic fields in the ambient medium and dense cloud, respectively. The spectral index of the emission α , where $S_\nu \propto \nu^{-\alpha}$, is assumed to be constant.

2. Radio Dark Clouds in the Inner Galaxy

Multi-wavelength images presented here are based on observations that have already been described elsewhere. The data that we have used are taken by Mopra telescope (Jones et al. 2011), Green Bank Telescope (GBT) of the National Radio Astronomy Observatory¹ (NRAO), (Law et al. 2008), Very Large Array (VLA) (Yusef-Zadeh et al. 2004), Antarctic Submillimeter Telescope and Remote Observatory (AST/RO) (Martin et al. 2004), IRAC on Spitzer Space Telescope (Arendt et al. 2008), SCUBA on James Clark Maxwell Telescope (Pierce-Price et al. 2000), Nobeyama Radio Observatory (NRO) (Tsuboi et al. 2011), and NICMOS of Hubble Space Telescope (HST) (Yusef-Zadeh et al. 2001). We present below multi-wavelength observations of five sources toward the inner Galaxy.

G359.75–0.13: Figure 1a shows the distribution of velocity integrated HCN (1-0) line emission from G359.75-0.13 which runs for $\sim 20'$ parallel to the Galactic plane (Jones et al. 2011)). This cloud is part of a layer of molecular gas associated with the central molecular zone. This elongated cloud is detected at mid-IR and submm images as an IRDC (Molinari et al. 2011; Arendt et al. 2008; Yusef-Zadeh et al. 2009). Figure 1b shows the radio continuum counterpart to the molecular cloud at 3.5 cm. A dearth of emission coincides with the cloud tracing HCN line emission. Figure 1c shows a composite color image of HCN (1-0) emission and 3.5 cm continuum image. Radio continuum emission is present to the north and south of the elongated molecular gas layer. To determine the anti-correlation between radio continuum and molecular line emission, cross cuts along a line drawn on Fig. 1a are made across the HCN and 3.5 cm radio continuum images and are presented in Figure 1d. The deficiency in the flux density of radio continuum emission is ~ 0.1 Jy implying that the depth of the ionized gas and molecular gas is similar to each other. These images demonstrate a clear anti-correlation in the distribution of molecular gas that is detected as an IRDC and radio dark cloud. The cross cuts combined with images of this cloud at radio and millimeter wavelengths suggest that the ionized and molecular gas in G359.75–0.13 are in the same environment, most likely in the Galactic center region. This is because diffuse radio continuum emission from the Galactic center is much stronger than in the Galactic disk.

G0.13-0.13 and the Radio Arc: Adjacent to the nonthermal filaments of the Arc near galactic longitude $\sim 0.2^\circ$ lies the molecular cloud G0.13-0.13 We compare the distribution of radio continuum and molecular line emission from G0.13-0.13. Figure 2a-b show the distributions of a 20cm continuum emission and integrated intensity of HCN (1-0) line,

¹The National Radio Astronomy Observatory is a facility of the National Science Foundation, operated under a cooperative agreement by Associated Universities, Inc.

respectively. The vertical filaments associated with the radio Arc are known to be magnetized structures running perpendicular to the Galactic plane. A 3.5cm image of the same region mapped by the GBT shows similar morphology to that of the 20cm continuum image. Using HCN line intensity and 3.5 cm continuum images, Figure 2c shows cross cuts, along a line drawn on Fig. 2b, demonstrating the depression in the continuum flux across the length of the cloud. The dip at the location of G0.13-0.13 corresponds to ~ 700 mJy at 3.5 cm. The molecular cloud G0.13-0.13 is surrounded by vertical nonthermal filaments of the Arc to the east (Yusef-Zadeh et al. 1987) and to the west of G0.13-0.13 (Reich 2003). The images and cross cuts made from HCN line and radio continuum data show anti-correlation between molecular line and radio continuum distributions. The largest deficiency of radio continuum emission is located where molecular line emission peaks. These intensity profiles imply the interaction of nonthermal radio filaments and G0.13-0.13 and are consistent with earlier studies measurements (Tsuboi et al. 1997). The flux of the continuum emission at 3.5cm is reduced by a factor 2 where the molecular cloud G0.13-0.13 is located. This implies that the region of nonthermal emission surrounding RDC is twice the depth of the molecular cloud.

G359.16–0.04 and the Snake Filament: One of the most prominent nonthermal filamentary structure in the Galactic center region is the Snake filament which extends for more than $20'$ and runs almost perpendicular to the Galactic plane (e.g., Gray et al. 1995). Figure 3a shows the northern half of this striking filament terminating at the radio continuum source G359.16-0.04 (Uchida et al. 1996). This 6cm continuum image shows two dark features RDC-1 and RDC-2 to the E. and W. edges of the extended continuum source giving the appearance of a “butterfly”. RDC-2 lies to the north of the well-known radio jet 1E1740-2942 (Mirabel et al. 1992). Given that the 6cm data is produced by the VLA and that incomplete uv coverage may be responsible for producing dark features, Figure 3b shows a grayscale 3.5cm continuum emission mapped by the GBT. We note that the dark features are also identified in single dish observations, thus establishing the reality of RDCs in interferometric images.

Contours of integrated emission of CO (4-3) line are superimposed on the 6cm continuum image, as shown in Figure 3c. Given the mismatch between the $2'$ resolution of molecular line data based on AST/RO observations and radio continuum data, the distribution of molecular gas is similar to that of dark radio clouds. The continuum image reveals detailed morphological structures of a giant molecular cloud on arcsecond spatial resolution especially at the boundary of the molecular cloud near the continuum source. We also made cross cuts at $b=-3' 45''$ across the 6cm and molecular line images, as shown on Figure 3d. The cross cuts show two peaks of molecular line emission coinciding with two dips in the 6cm image with deficient radio flux of roughly 400 and 300 mJy. These dips correspond to RDC-1 and

RDC-2, and imply that the diameters of RDC-1 and RDC-2 are roughly 4/5 and 3/5 of the depth of the ionized medium surrounding the cloud.

G0.6-0.0 Sgr B2: The Sgr B2 cloud is a well-studied giant molecular cloud which lies near the Galactic center (Reid et al. 2009) and is part of a continuous dust ridge that is viewed in absorption at mid-IR wavelengths (Lis & Carlstrom 1994; Molinari et al. 2011). Figure 4a shows the IRDC associated with Sgr B2 to the N. and NE of the cluster of stars and the nebula. Figure 4b,c show the distribution of 20 and 6cm continuum emission from the same region, respectively. The brightness of the 20cm continuum emission is saturated to bring out an elongated dark feature near $b = 0^\circ$. Radio continuum images show RDC-1 which appears to coincide with the southern edge of IRDC that surrounds the cluster of UC HII regions in Sgr B2 (De Pree et al. 2000). We also note a decrease in the radio flux at 6 and 20cm between Sgr B2 and the isolated radio continuum feature G0.73-0.10. However, the image quality in this region is poor, thus may show artifacts. Cross cut plots along a line drawn on Fig. 4c across the RDC-1 are made using the 6cm continuum and $450\mu\text{m}$ images. The profiles of emission, as shown in Figure 4d, show flux deficiencies of 5 and 2 mJy which imply that the depths of the ionized gas for the two dips are similar to and twice larger than those of molecular gas, respectively. Because of the large number of bright compact HII regions in Sgr B2, the cross cuts also show fluctuations due to emission from individual compact sources.

Sgr A East SNR & Sgr A West: Given its gaseous environment with a strong radiation field, the inner ten parsecs of the Galactic center is an excellent site to search for RDCs tracing molecular clouds that interact with the strong radiation field or with expanding supernova remnants. The strong radiation field in the Galactic center produces a thick layer of ionized gas at the edge of dark clouds. One of the most prominent giant molecular clouds in the Galactic center is the 50 km s^{-1} G0.02-0.07. This cloud is physically interacting with the expanding shell of the Sgr A East SNR G0.0+0.0 which is thought to lie near the Galactic center (e.g., Tsuboi et al. 2011). This complex region is also the site of young massive star formation as a chain of compact HII regions that lie to the east of the Sgr A East remnant. Figures 5a-b show the inner $4'$ of the Galactic center at 6cm hosting the shell-type SNR G0.0-0.0 and four compact HII regions A-D at its eastern boundary (Zylka et al. 1992). The 1.3mm continuum distribution traces dust emission from the 50 km s^{-1} molecular cloud. We note several dark features RDC-1 to 4 surrounding the SNR shell of Figure 5a, all of which coincide with dust and molecular features (Tsuboi et al. 2011). The largest scale dark cloud RDC-1 is noted to the NE of the chain of HII regions where we note an oval-shaped structure with an extent of $2' \times 1'.1$. Figure 5c shows contours of integrated emission of SiO (2-1) superimposed on the 6cm image, supporting the suggestion that RDC-1 coincides with an oval-shaped molecular gas. Another chain of HII regions to the NE of RDC-1 near

$\delta = -28^{\circ} 58'$ might be associated with a second site of star formation in this cloud. To estimate the level at which the continuum emission is suppressed, Figure 5d shows cross cuts of RDC-3 made at 1.3mm and 6cm, supporting a clear anti-correlation between dust and radio continuum emission. The largest deficient flux at 6cm is 25 mJy implying that the size of the hot plasma is twice the size of the molecular cloud.

On a smaller scale, the inner pc of the Galactic center hosts diffuse ionized gas Sgr A West orbiting the massive black hole (e.g., Ferriere et al. 2012). Sgr A West consists of three arms of ionized gas and is surrounded by the Circumnuclear molecular ring (CMR). Figure 5e,f show a 3.5cm and $1.87\mu\text{m}$ continuum images of the eastern half of Sgr A West whereas Figures 5g show molecular H2 1-0 S(1) counterparts (Yusef-Zadeh et al. 2001). Several dark features are noted in the 3.5cm continuum image, especially in the region between the N. and E. arms. It turns out RDC-1 and RDC-2 lying between the two arms coincide with an extinction feature, as revealed in Figure 5h where a drop in stellar density is noted. Cross cuts across the 3.5cm and H2 images show that the H2 emission coincides with a dip in the continuum peak at 3.5cm. The deficient flux at 3.5cm suggests that the depth of the ionizing gas is similar to that of the molecular gas. From equation (2), the depth of the cloud is estimated to be 0.11 pc if $n_e \sim 5000 \text{ cm}^{-3}$ and $T_e \sim 6000\text{K}$.

The association of a "tongue" of neutral gas (RDC-3), an extinction cloud with the N. arm of Sgr A West (Jackson et al. 1993; Yusef-Zadeh et al. 2001), as well as the association of the E. arm with neutral gas suggest that there is considerable molecular gas in the ring and that the arms of Sgr A West trace the ionized surface of neutral clouds. If these clouds are massive, the presence of molecular gas inside the CMR can have important consequences in the formation of stars and the dynamics of stars near Sgr A*.

Conclusions: We have presented five examples of dark features in radio continuum images of molecular complexes toward the inner Galaxy. We illustrated that these dark features are anti-correlated with molecular line and dust emission, thus implying that cold gas associated with radio continuum features can be detected in radio images. Given the new generation of radio telescopes with their broad band capability, future continuum measurements could potentially be effective in identifying cold gas clouds in star forming sites in the local and distant universe. Some of the dark radio clouds are surrounded by nonthermal radio emission, thus, radio continuum imaging can identify the interaction of nonthermal particles from radio jets or jet-driven outflows or supernova remnants with the cold ISM or the IGM. Lastly, RDCs can potentially be used as OFF positions in total power technique of observations with radio telescopes.

Acknowledgments: I am grateful to M. Wardle, D. Roberts, R. Arendt, W. Cotton, M. Royster, M. Tsuboi and other colleagues for discussions and for providing me with their data

over the years. This work is partially supported by the grant AST-0807400 from the NSF.

REFERENCES

- Andersen, L. D., Snowden, S. L. & Bania, T. M. 2010, *ApJ*, 721, 1319
- Arendt, R. G., Stolovy, S. R., Ramirez, S. V. et al. 2008, *ApJ*, 804,
- De Pree, C.G., Wilner, D.J., Goss, W.M. et al. 2000, *ApJ*, 540, 308
- Egan, M. P., Shipman, R. F., Price, S. D. et al. 1998, *ApJ*, 494, 199
- Ferriere, K. 2012, *A&A*, 540, 50
- Gray, A.D., Nicholls, J., Ekers, R.D. & Cram, L.E. 1995, *ApJ*, 448, 164
- Jackson, J. M., Geis, N., Genzel, R. et al. 1993, *ApJ*, 402, 173
- Law, C. J., Yusef-Zadeh, F., Cotton, W. D., & Maddalena, R. J. 2008, *ApJS*, 177, 255
- Lang, C. C., Goss, W. M., Cyganowski, C., & Clubb, K. I. 2010, *ApJS*, 191, 275L
- Jones, P. A., Burton, M. G., Tothill, N. F. H. & Cunningham, M. R. 2011, *MNRAS*, 411, 2293
- Lis, D. C. & Carlstrom, J. E. 1994, *ApJ*, 424, 189
- Martin, C. L., Walsh, W., Xiao, K. et al. 2004, *ApJS*, 153, 395
- Mirabel, I. F., Rodriguez, L. F., Cordier, B. et al. 1992, *ApJ*, 358, 215
- Molinari, S., Bally, J., Noriega-Crespo, A., *et al.* 2011, *ApJ*, 735, 33
- Morris, M. & Serabyn, E. 1996, *ARA&A*, 34, 645
- Nord, M. E., Lazio, T. J. W., Kassim, N. E., Hyman, S. D., LaRosa, T. N., et al. 2004, *AJ*, 128, 1646
- Oka, T., Geballe, T. R., Goto, M., Usuda, T., & McCall, B. J. 2005, *ApJ*, 632 882
- Pierce-Price, D., Richer, J. S., Greaves, J. S., *et al.* 2000, *ApJ*, 545, 121
- Reich, W. 2003, *A&A*, 401, 1023

- Reid, M. Menten, K. M., Zheng, X. W. et al. 2009, ApJ, 705, 1548
- Sawada, T., Hasegawa, T., Handa, T. & Cohen, R. J. 2004, MNRAS, 349, 1167
- Tsuboi, M., Tadaki, K., Miyazaki, A. & Handa, T. 2011, PASJ, 63, 763
- Tsuboi, M., M., Ukita, N., & Handa, T. 1997, ApJ, 481, 263
- Uchida, K. I., Morris, M., Serabyn, E., Güsten, R. 1996, ApJ, 462, 768
- Yusef-Zadeh, F., Hewitt, J. W., & Cotton, W. 2004, ApJS, 155, 421
- Yusef-Zadeh, F., Hewitt, J. W., Arendt, R. G. et al. 2009, ApJ, 702, 178
- Yusef-Zadeh, F., Hewitt, J. W., Wardle, M. et al. . 2012, ApJ, submitted
- Yusef-Zadeh, F. and Morris, M. 1987, ApJ, 322, 721
- Yusef-Zadeh, F., Stolovy, S. R., Burton, M. et al. 2001, ApJ, 560, 749
- Zylka, R., Mezger, P. G. & Lesch, H. 1992, A&A, 261, 119

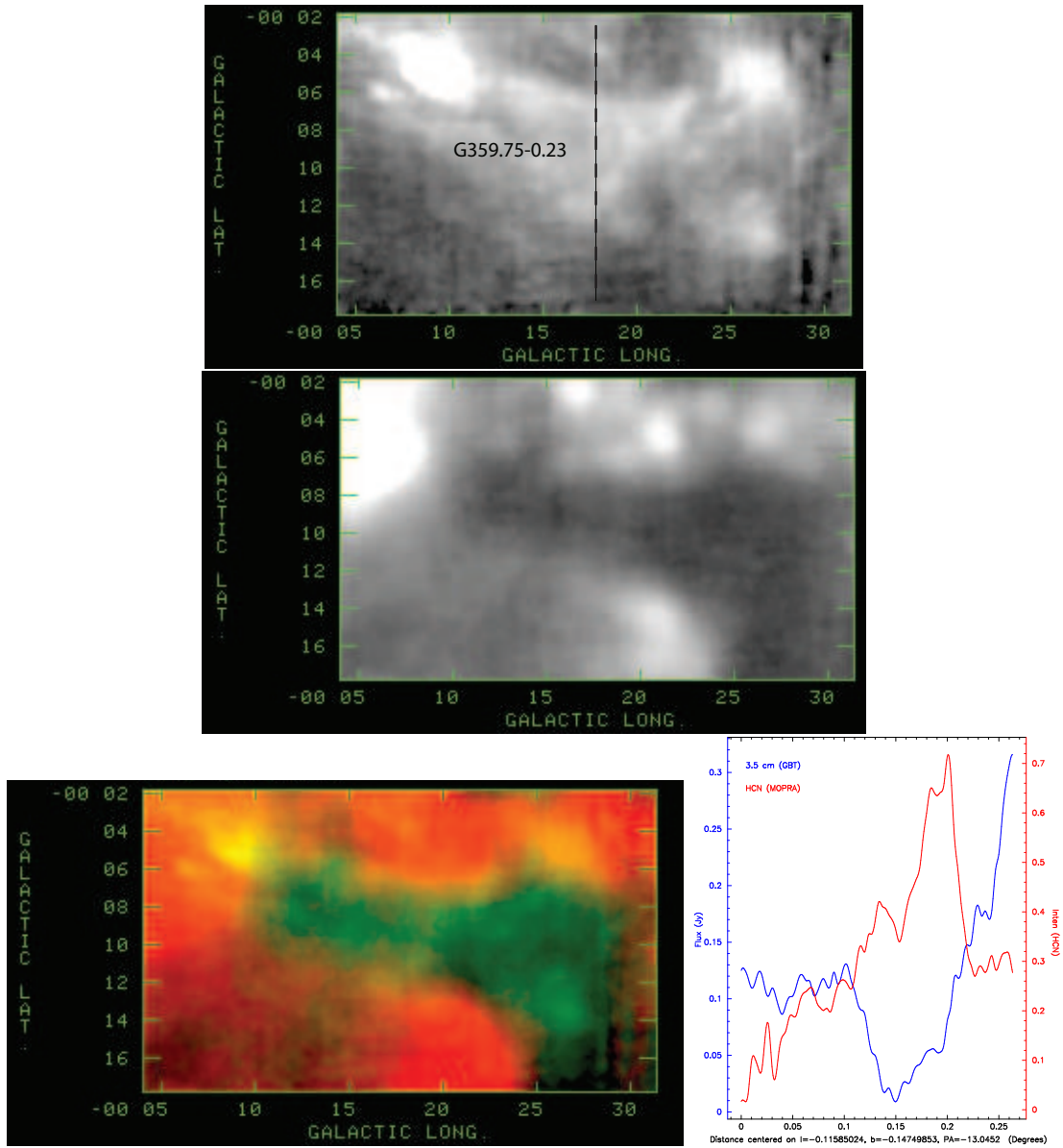


Fig. 1.— (a) *Top* - The integrated greysclae emission of the HCN (1-0) line from IRDC G359.75-0.13 over velocities between -22.9 and -8.5 km s^{-1} based on MOPRA observations with a resolution of $\sim 39''$. (b) *Middle* - Similar to (a) except showing the distribution of radio continuum emission at 3.5 cm based on GBT observation with a spatial resolution of $88''$. (c) *Bottom* - A color composite image showing (a) and (b) in red and green, respectively. (d) *Right* - A Cross cut, as drawn on (a), made at constant $l=16' 36''$ showing the intensity profiles of HCN line emission in red and and of 3.5 cm continuum data in blue.

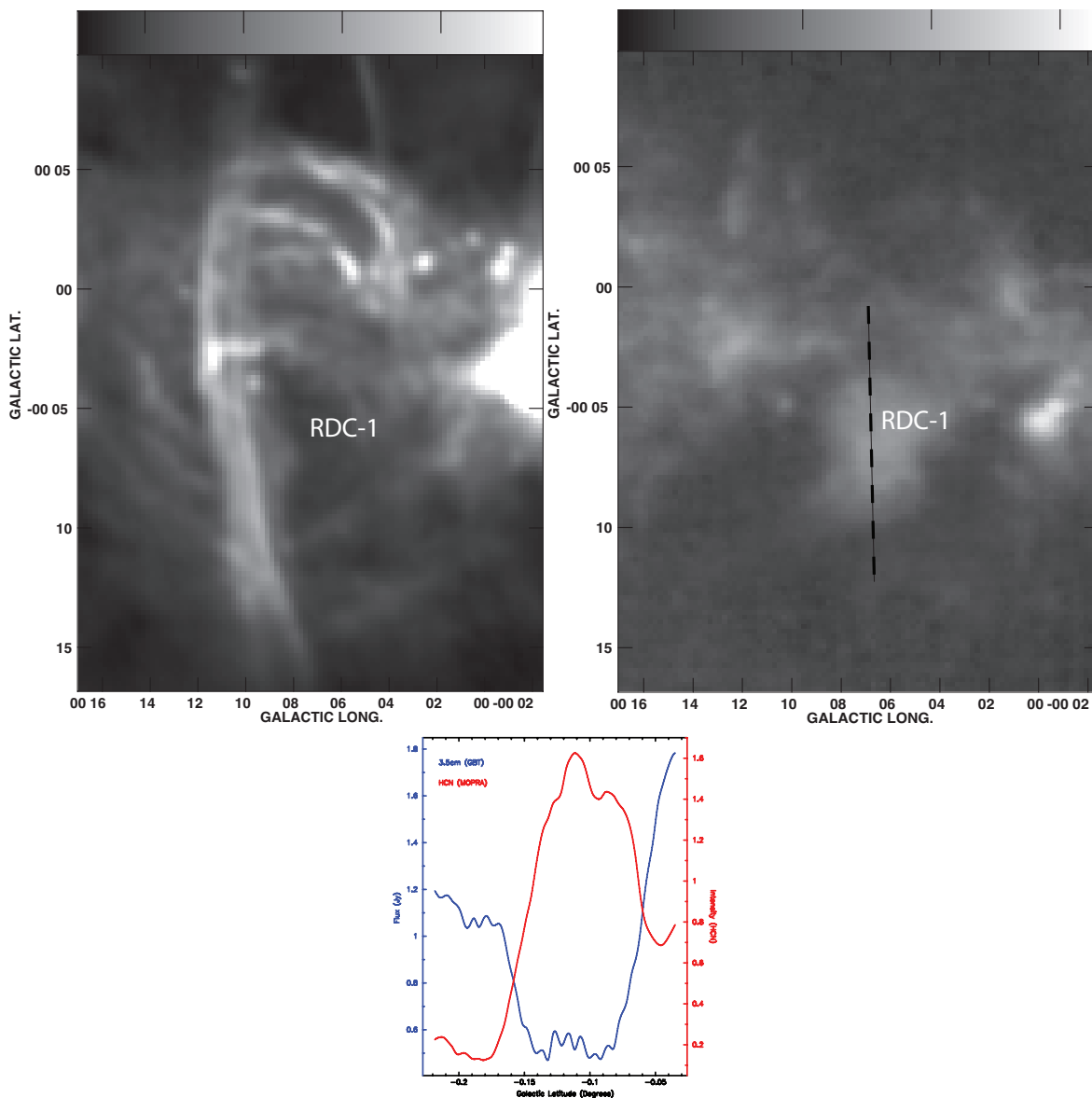


Fig. 2.— (a) *Top Left* - A grayscale continuum image of the radio Arc at 20cm with a resolution of 30". (b) *Top Right* - The integrated emission of the HCN line over velocities between 0 and 50 km s⁻¹ with a spatial resolution of 39" (Jones et al. 2011). (c) *Bottom Left* - Cross cuts aslong a line drawn on (b) are made at constant $l \sim 6'.1$ showing the profiles of HCN line emission in red and of 3.5 cm continuum emission based on GBT observation in blue.

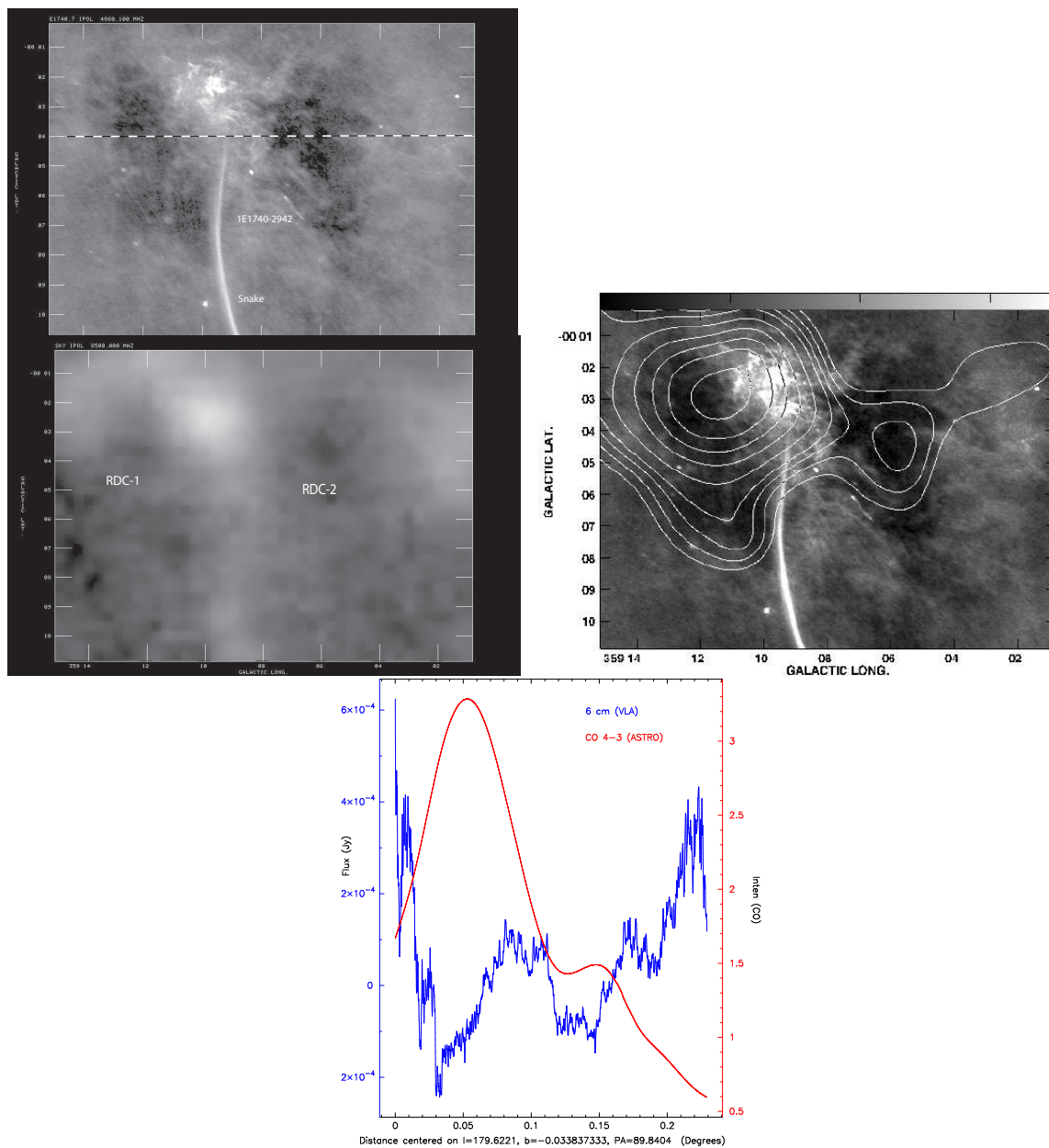


Fig. 3.— (a) *Top Left* - A grayscale 6cm continuum image of the snake filament based on observations taken with all four configurations of the VLA with a resolution of $3.72'' \times 1.86''$ and rms noise $10\mu\text{Jy}$. (b) *Bottom Left* - Similar to (a) except that a 3.5 cm continuum image taken with the GBT with a spatial resolution of $89''$. (c) *Top Right* - A weighted average contours of CO (4-3) line emission integrated between -150.5 and -140.5 km s^{-1} with a resolution of $\sim 2'$ superimposed on (a). (d) *Bottom* - Cross cuts along a line drawn on (a) at $b=-3' 45''$ show two CO peaks and two 6cm continuum dips, corresponding to RDC-1 and RDC-2. The VLA image at 6cm is primary beam corrected.

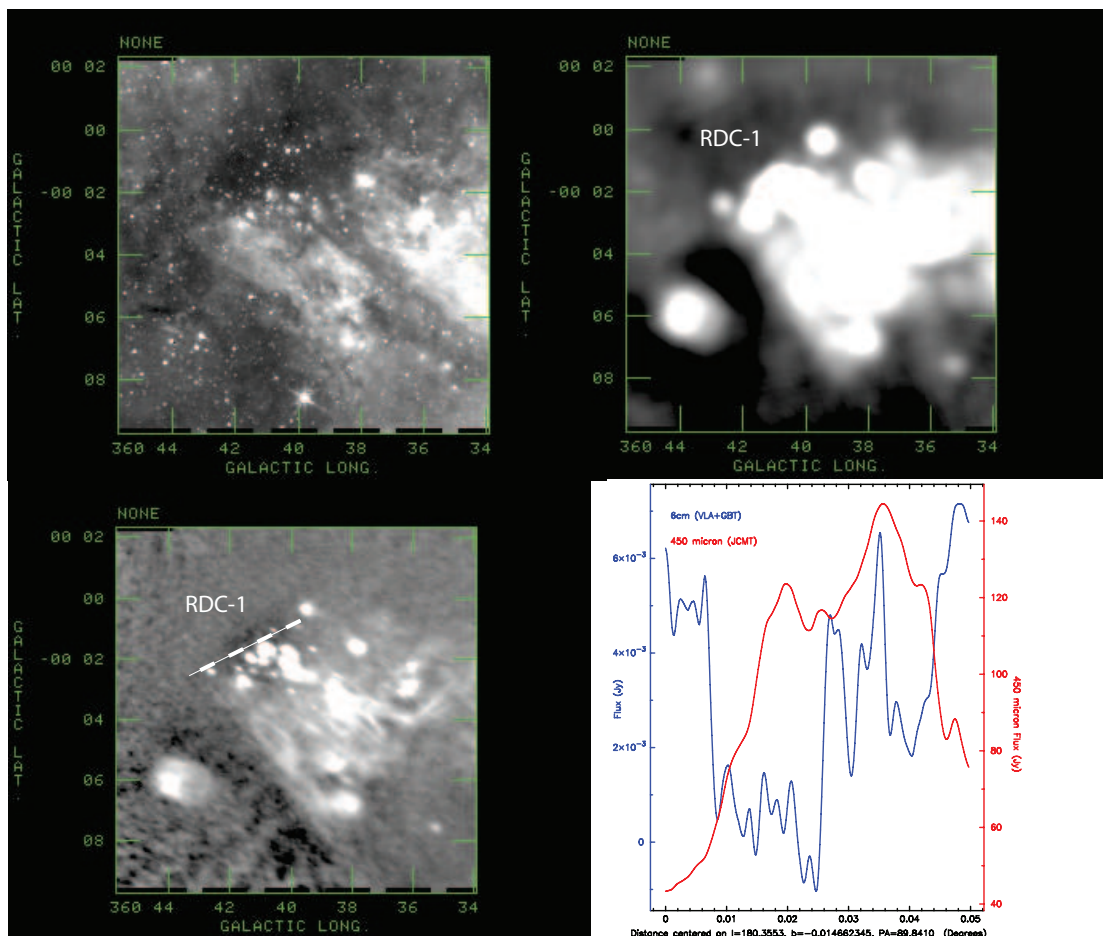


Fig. 4.— (a) *Top Left* - An IRAC image of Sgr B2 at $8\mu\text{m}$ with a resolution of $\sim 2''$ (b) *Top Right* - A continuum image of Sgr B2 at 20cm based on combining data taken from the C and D configurations of the VLA and the GBT before the image was convolved to a resolution of $30''$. (c) *Bottom Left* - Similar to (b) (both VLA and GBT data combined) but at a resolution of $10.8'' \times 5.5''$ (d) *Bottom Right* - Cross cuts centered at $l = 41' 15'' b = -1' 12''$ along a line drawn on (c) show profiles of emission at $450\mu\text{m}$ and 6cm in blue and red, respectively.

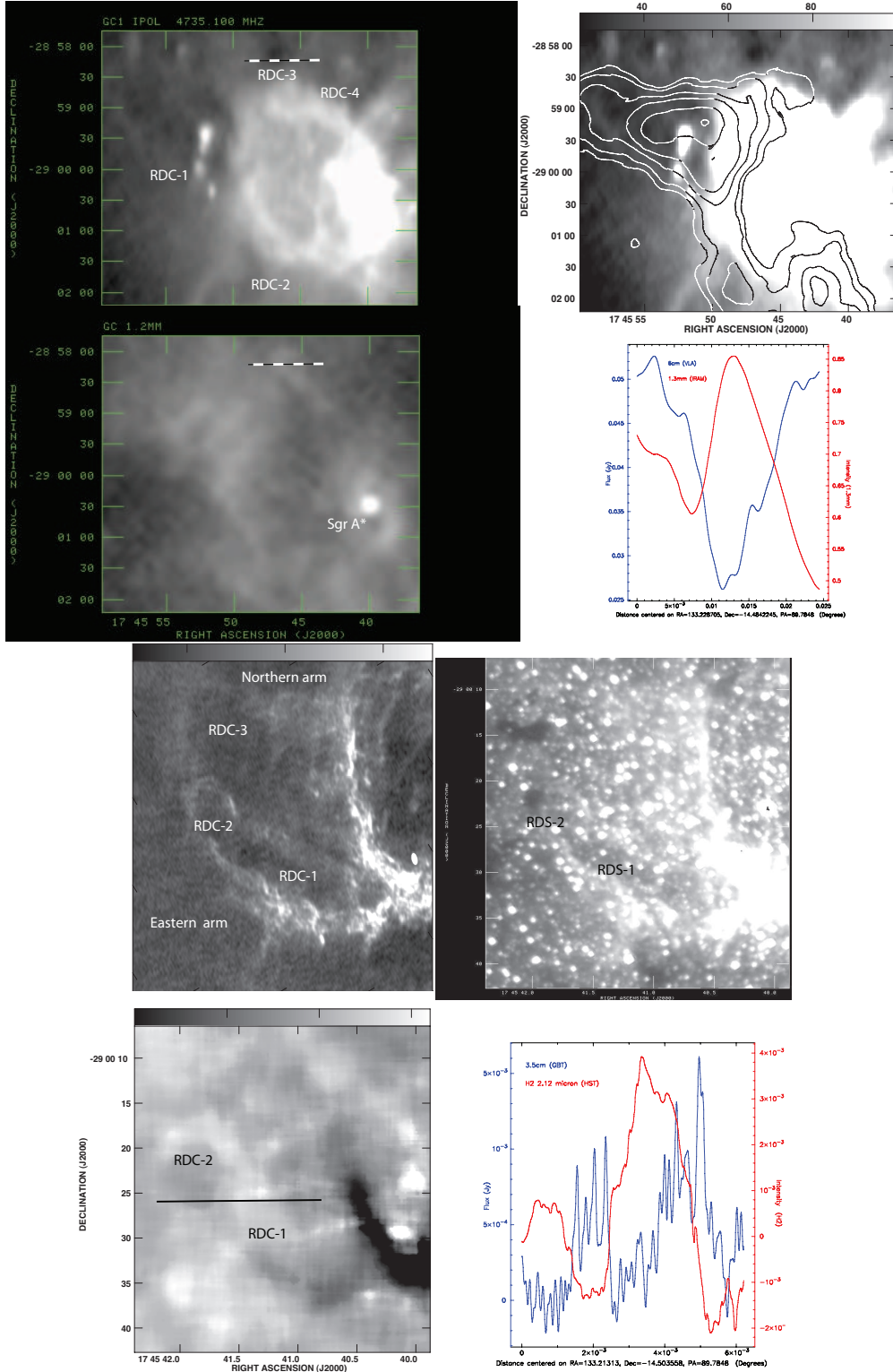


Fig. 5.— (a-d) Top 4 - Radio continuum of Sgr A East at 6cm, the distribution of dust emission at 1.3 mm, contours of SiO (2-1) line emission superimposed on a 6cm continuum image and the cross cuts at 1.3mm and 6cm at the position of RDC-3 along the line drawn on (a) and (b). (e-h) Bottom 4 - Radio continuum at 3.5cm with a resolution of $0.45'' \times 0.22''$, stellar subtracted H2 1-0 S(1) emission at $2.12\mu\text{m}$, an image of $1.87\mu\text{m}$ emission from stars and ionized gas, the cross cuts along the line drawn on (f) show the emission profiles of